

Numerical study of the influence of ZnTe thickness on CdS/ZnTe solar cell performance^{*}

Othmane Skhouni¹, Ahmed El Manouni^{1,2,a}, Bernabe Mari², and Hanif Ullah²

¹ Laboratoire de Physique de l'Atmosphère et Modélisation (LPAM), Université Hassan II, Faculté des Sciences et Techniques, BP 145 Mohammedia, Morocco

² Departament de Física Aplicada-ETSED, Universitat Politècnica de València, Camí de Vera s/n 46022 València, Spain

Received: 17 July 2015 / Received in final form: 30 August 2015 / Accepted: 2 September 2015
Published online: 3 May 2016 – © EDP Sciences 2016

Abstract. At present most of II–VI semiconductor based solar cells use the CdTe material as an absorber film. The simulation of its performance is realized by means of various numerical modelling programs. We have modelled a solar cell based on zinc telluride (ZnTe) thin film as absorber in substitution to the CdTe material, which contains the cadmium element known by its toxicity. The performance of such photovoltaic device has been numerically simulated and the thickness of the absorber layer has been optimized to give the optimal conversion efficiency. A photovoltaic device consisting of a ZnTe layer as absorber, CdS as the buffer layer and ZnO as a window layer was modelled through Solar Cell Capacitance Simulator Software. Dark and illuminated I - V characteristics and the results for different output parameters of ZnO/CdS/ZnTe solar cell were analyzed. The effect of ZnTe absorber thickness on different main working parameters such as: open-circuit voltage V_{oc} , short-circuit current density J_{sc} , fill factor FF, photovoltaic conversion efficiency η was intensely studied in order to optimize ZnTe film thickness. This study reveals that increasing the thickness of ZnTe absorber layer results in higher efficiency until a maximum value and then decreases slightly. This maximum was found to be 10% at ZnTe optimum thickness close to 2 μm .

1 Introduction

Owing to its wide band gap of 2.23–2.28 eV at room temperature [1,2], high absorption coefficient close to 10^5 cm^{-1} and low electron affinity 3.73 eV [3]. Zinc telluride (ZnTe) is one of the most promising II–VI semiconductor candidates for the development of low-cost and high-efficiency thin film solar cells [4]. Furthermore, ZnTe is a p -type semiconductor which can form with n -type CdS thin layer a p - n junction more useful for photovoltaic solar energy conversion because it undertakes a high-energy part of the solar spectrum in the conversion process. However, due to its high band gap ZnTe cannot absorb enough photons with energy lies in visible region limiting therefore the conversion efficiency. To remedy this II–VI semiconductors with an intermediate band (IB) located inside the semiconductor bandgap seem to be the appropriated solution for increasing the conversion efficiency. Indeed the intermediate band solar cells (IB-SCs) offer another

concept of absorption based on multi-photon absorption with assistance of an IB situated in the bandgap of an active semiconductor [5,6], the IB must be partially filled to allow absorption of photons with energy below the energy bandgap. It is possible for ZnTe to generate an IB by doping with oxygen forming ZnTe:O alloy which is an attractive material for photovoltaic devices [7]. This kind of solar cells allowed increasing the limiting conversion efficiency of single gap semiconductor based solar cells from 40.7% to 63.2% for IBSCs [5,8–10].

Most of II–VI semiconductor based solar cells use the CdTe thin film as an absorber material with thickness more than 5 μm and the obtained theoretical and measured conversion efficiencies ranging 16–25% [11,12] and 8–16% [13], respectively. In our case we suggest replace the CdTe material usually used as an absorber in solar cells by ZnTe layer eliminating therefore the cadmium element which is well known by its toxicity. So this paper reports on modelling a ZnO/CdS/ZnTe solar cell and simulating of its performance using solar cell capacitance simulator software (SCAPS). A numerical study of the effect of ZnTe thickness on the main working parameters such as, open-circuit voltage V_{oc} , short-circuit current density J_{sc} , fill factor FF and photovoltaic conversion efficiency η , has been carried out.

^a e-mail: elmanouni123@gmail.com

^{*} Contribution to the topical issue “Materials for Energy Harvesting, Conversion and Storage (ICOME 2015) – Elected submissions”, edited by Jean-Michel Nunzi, Rachid Bennacer and Mohammed El Ganaoui

2 Basic equations

The numerical SCAPS software is a one dimensional solar cell simulation program. It was designed as a general polycrystalline thin-film device simulator, and has been used for modelling solar cells based on conventional thin film semiconductors such CIGS and CdTe [14] or new promising materials like S_nS [15]. Also it offers possibility to set a composition grading of various material parameters. SCAPS program allows mainly:

- to estimate the steady-state band diagram, recombination profile, carrier transport in 1D,
- to calculate the recombination currents using the Shockley-Read-Hall (SRH) model for bulk and interface defects,
- to determinate spectral response, J_{sc} - V , C - V , C - f and Q - V . Each measurement can be calculated for light and/or dark conditions and as a function of temperature,
- to simulate IB solar cells by modifying the absorption coefficient of the absorber layer to take into account the absorption of photons with energy below the bandgap energy.

In order to simulate the modelled ZnO/CdS/ZnTe solar cell, the SCAPS software allows solving the basic semiconductor equations: the Poisson equation and the continuity equations.

- Poisson equation:

$$\nabla(\hat{E}) = \frac{q}{\epsilon} (p - n + N_D^+ - N_A^-), \quad (1)$$

- continuity equations:

$$\frac{\partial n}{\partial t} = \frac{1}{q} \nabla(J_n) + G_n - R_n, \quad (2)$$

$$\frac{\partial p}{\partial t} = \frac{1}{q} \nabla(J_p) + G_p - R_p, \quad (3)$$

- transport equations:

$$J_n = q (\mu_n n \hat{E} + D_n \nabla n), \quad (4)$$

$$J_p = q (\mu_p p \hat{E} + D_p \nabla p), \quad (5)$$

- built-in voltage p - n homojunction:

$$V_0 = \frac{kT}{q} \ln \left(\frac{N_A N_D}{n_i^2} \right), \quad (6)$$

- general ideal diode current equation:

$$I = I_0 \left(\exp \left(\frac{qV}{nAKT} \right) - 1 \right) - I_{ph}, \quad (7)$$

where ϵ is the permittivity of the absorber, E is the electrical field, q is elementary charge, N_D (N_A) is donor (acceptor) concentration, G (R) is carrier generation

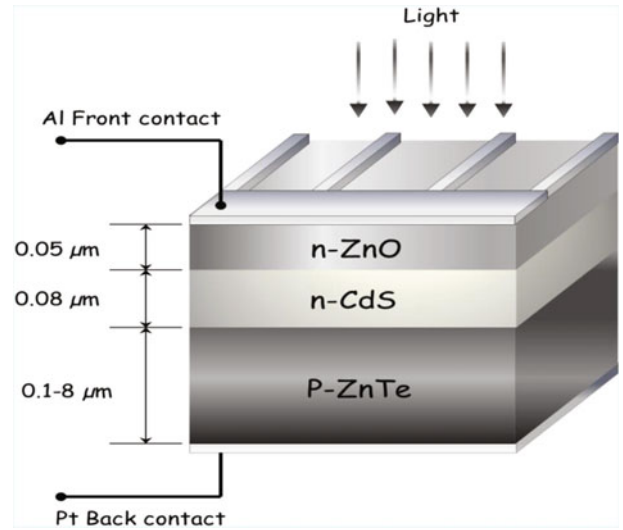


Fig. 1. Schematic structure of CdS/ZnTe solar cell in substrate configuration.

(recombination) rate, n (p) is density of electrons (holes), J_n (J_p) is current density of electron (holes), K is Boltzmann constant, T is the temperature, I_{ph} is the photoelectric current and I_0 is the reverse saturation current given by: $I_0 = Aq \left[\frac{D_p P_{n0}}{L_p} + \frac{D_n P_{p0}}{L_n} \right]$, where D is the diffusion constant and L is the diffusion length of each carrier type, P_{n0} and n_{p0} are the majority carrier concentrations on the p and n side. A is the diode quality factor. The value of A depends on the current transport. For injection/diffusion mechanism $n = 1$ and for recombination mechanism $n = 2$.

3 Design of ZnTe-based solar cell

The schematic of the ZnTe thin film solar cell used in the simulation with ZnO/CdS (n -type)/ZnTe (p -type)/metal structure is shown in Figure 1. The p -ZnTe film is used as an absorber layer, n -CdS as a buffer and ZnO as a window. The design is presented in the substrate configuration and the illuminated side of the modelled CdS/ZnTe solar cell is the ZnO window.

4 Input parameters

In order to simulate the photovoltaic characteristics of the solar cell device presented above several parameters concerning the absorber layer, the buffer and window material must be defined. Some of them have been calculated and the others were either extracted from literature or from the database of SCAPS program.

4.1 Front and back contacts and surfaces

In general, contacts are assumed ohmic, or depending on the focus of the modelling, assigned a Schottky barrier

Table 1. Basic parameters used in simulation of ZnTe based solar cell characteristics (Refs. [1, 12, 16, 18, 19]).

Contact parameters	Front contact (Al)		Back contact (Pt)
Work function Φ (eV)	4.45		5.40
Surface recombination velocity of electrons S_e (cm/s)	10^7		10^7
Surface recombination velocity of holes S_h (cm/s)	10^7		10^7
Reflectivity R_f	0.05		0.8
Layer properties	ZnTe (<i>p</i> type)	CdS (<i>n</i> type)	ZnO (TCO)
Thickness (μm)	0.1–8	0.08	0.05
E_g (eV)	2.19	2.43	3.37
Electron affinity (eV)	3.73	4.0	4.45
Dielectric constant	10.3	9.35	9.00
CB effective density of state for electron (cm^{-3}) N_c	1.176×10^{18}	1.758×10^{18}	2.949×10^{18}
VB effective density of states (cm^{-3}) N_v	1.166×10^{19}	1.469×10^{19}	1.137×10^{19}
Electron thermal velocity (cm/s)	3.24×10^7	2.83×10^7	2.38×10^7
Hole thermal velocity (cm/s)	1.51×10^7	1.39×10^7	1.52×10^7
Electron mobility μ_n ($\text{cm}^2/\text{v s}$) à 300 K	330	100	100
Hole mobility μ_h ($\text{cm}^2/\text{v s}$) à 300 K	80	25	25
Shallow uniform donor density N_D (cm^{-3})	0	1.0×10^{18}	1.0×10^{18}
Shallow uniform acceptor density N_A (cm^{-3})	2.16×10^{19}	0	0

height consistent with experimental observations. The front and back contacts of the modelled CdS/ZnTe solar cell are in aluminium and platinum respectively. The back contact plays a key role on the performance of solar cells. It must have a work function greater or equal to sum of band gap energy and electron affinity of ZnTe layer. The reflexion at the back surface has only a minor influence on the short-circuit current density (J_{sc}), however this influence only become noticeable if the absorber is chosen to be fairly thin. At the front contact the multiplicative reflexion factor is often considered constant (i.e., reflexion $R_F = 5\%$). External quantum efficiency, EQE, is then reduced by this factor and, if interference effects and recombination losses are neglected, it will expected that EQE spectrum shows a maximum response at intermediate wavelengths around $1 - R_F = 95\%$.

4.2 Material parameters

The input parameters of ZnTe, CdS and ZnO layers are shown in Table 1. Some of them were calculated; the others were either extracted from our previous work [16] or from literature or from the SCAPS database.

The effective density of states for electron, N_c , was calculated using the following expression:

$$N_c = 2 \left(\frac{2\pi m_e^* K T}{h^2} \right)^{\frac{3}{2}}, \quad (8)$$

where m_e^* is the effective mass of electron given by $m_e^* = 0.13 m_0$, with m_0 is the free electron mass, T is the temperature, K is the Boltzmann constant and h is the Planck constant. The effective density of states for hole can be calculated from the relation (8) replacing the effective mass of electron by effective mass of hole, using $m_h^* = 0.6 m_0$.

4.3 Defect states

The SCAPS simulation program integrates for each layer two defect types: shallow level and deep defects. The first is defined as one shallow level completely ionized and it does not contribute to the recombination processes. The second can be represented by more than three deep levels governed by the Shockley-Read-Hall model [17]. Deep levels contribute to recombination in different interfaces and within layers and the charge of each level is defined by occupation of the level and its type (donor or acceptor or neutral). The energy distribution of these levels can be modelled either by a single level, uniform band, Gaussian band or exponential repartition. For simulation calculations we have introduced as input parameters relative to defect states capture cross sections for electron and hole, σ_e and σ_p , defect distribution $N_{\text{def}}(E)$ and total density of deep levels N_t . We have also assumed that defects in both CdS and ZnO layers are neutral deep levels with Gaussian distributions. For ZnTe absorber defects, we have introduced two uniform single levels of width about 0.51 and 0.60 eV due to the zinc vacancy defect [18].

5 Results and discussion

The main objective is at first to replace the CdTe absorber layer which often used as an absorber in solar cells by ZnTe film in order to eliminate the cadmium element and then make a numerical optimization of ZnTe thickness to realize economy of material. The obtained output parameters as function of ZnTe absorber thickness of the modelled ZnO/CdS/ZnTe solar cell are presented below. The ZnTe thickness was varied from 0.1 to 8 μm and the temperature is maintained at 300 K.

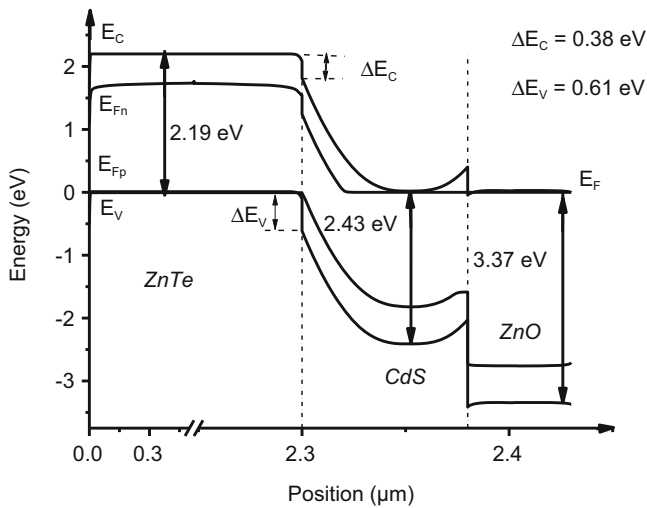


Fig. 2. Energy band diagram of ZnO/CdS/ZnTe solar cell at zero bias in the dark.

5.1 Energy band diagram

Figure 2 shows the energy band diagram generated by SCAPS for ZnO/CdS/ZnTe interfaces at zero bias in the dark with various positions within the cell layers. The band diagram is plotted for ZnTe absorber layer, CdS buffer and ZnO window thicknesses of about 2.3, 0.08 and 0.05 μm respectively. Also, the energy levels are shown with respect to the Fermi level, which is set to 0 eV in the band diagram. One can see that due to the high carrier concentration in the ZnTe layer there is no barrier at the CdS/ZnTe interface with a depletion region in CdS of 0.01 μm and not in ZnTe. A potential drop at the CdS/ZnTe interface is occurred with values of 0.38 and 0.61 eV in conduction and valence bands respectively. It is shown also that there is Schottky barrier at the back contact with height about approximately 0.5 eV which influences significantly the cell performance. Both the high bandgap of ZnTe absorber layer and contact properties are probably the reason for the highly calculated open circuit voltage of about 1.81 eV.

5.2 J-V characteristics

The obtained current-voltage characteristics of ZnTe based solar cell at dark and under illumination are shown in Figure 3. The ZnTe thickness was varied from 0.1 to 8 μm . J - V curves for ZnTe thicknesses higher than 2 μm tend to saturate at the same values (not shown here). In fact as can be already seen in Figure 3 the J - V curves for 1 and 2 μm are quite similar. Typical features of these characteristics are: the light and dark curves show a cross-over effect and an increasing of the current as the voltage increases. This indicates that the current depends on voltage and carrier transport mechanism.

The dark J - V curve is typical of a Schottky diode with a current minimum due to the minority carriers. Under illumination AM1.5 conditions the short circuit current

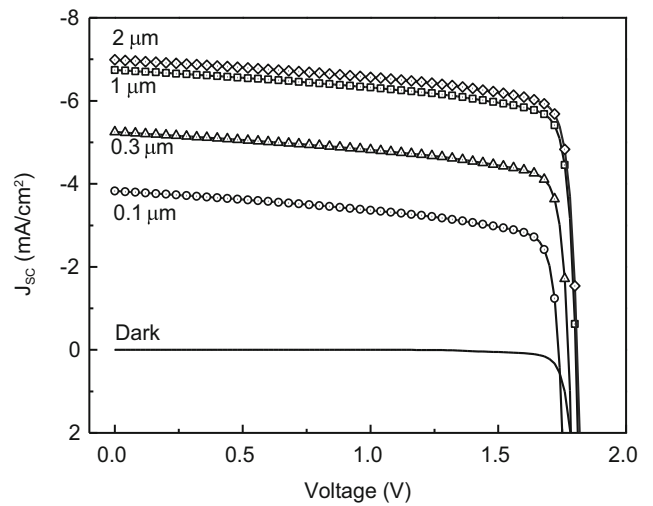


Fig. 3. Current-voltage characteristics of ZnTe based solar cell for different ZnTe thicknesses at the dark and under illumination AM1.5.

depends on the thickness of the absorber layer. As can be seen in Figure 3 the short circuit current increases with the thickness of the absorber layer reaching a maximum about 7 mA/cm^2 when the thickness of the absorber layer is 2 μm . Thicker absorber layers do not result in any enhancement of the short circuit current. Instead a slight drop of the short circuit current is observed due to the rise of the resistance of the overall device. Therefore it can be considered that the optimum thickness for the ZnTe absorber layer in the proposed device is about 2 μm .

5.3 External quantum efficiency

The influence of ZnTe absorber thickness on the spectral response of the modelled ZnO/CdS/ZnTe solar cell is shown in Figure 4. One can see that external quantum efficiency, EQE, and the long-wavelength spectral response decrease with decreasing of the ZnTe thickness. Therefore, insufficient absorption of photon is occurred in case of thinner ZnTe absorber because recombination losses at back surface became important as already observed on CdTe thin film based solar cells [12]. The spectral response spectrum can be divided in three regions: the first region localised between 480 and 620 nm corresponds to the absorption in ZnTe absorber, the second region with wavelength ranging 370–480 nm is relative to the absorption in CdS layer and the third region for wavelength values below 370 nm is attributed to the absorption in ZnO window. Additionally, the maximum of the uppermost curve corresponds to EQE of 74% which is lower than the expected value (95%).

5.4 Optimization of ZnTe thickness

In order to optimize the ZnTe absorber layer in the modelled solar cell device, the effect of ZnTe thickness

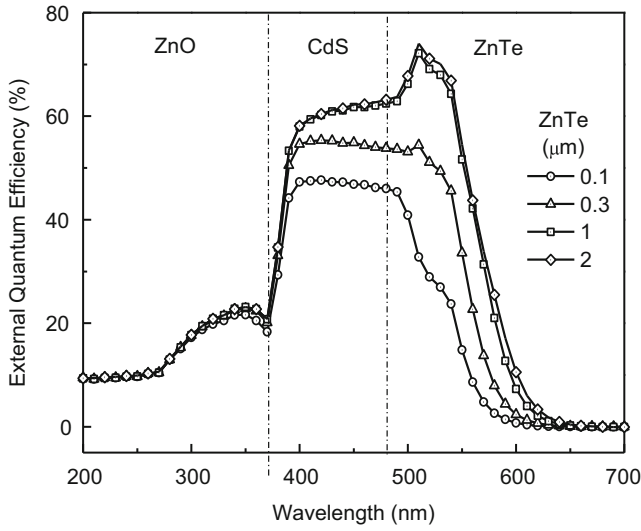


Fig. 4. Spectral response of ZnO/CdS/ZnTe solar cell.

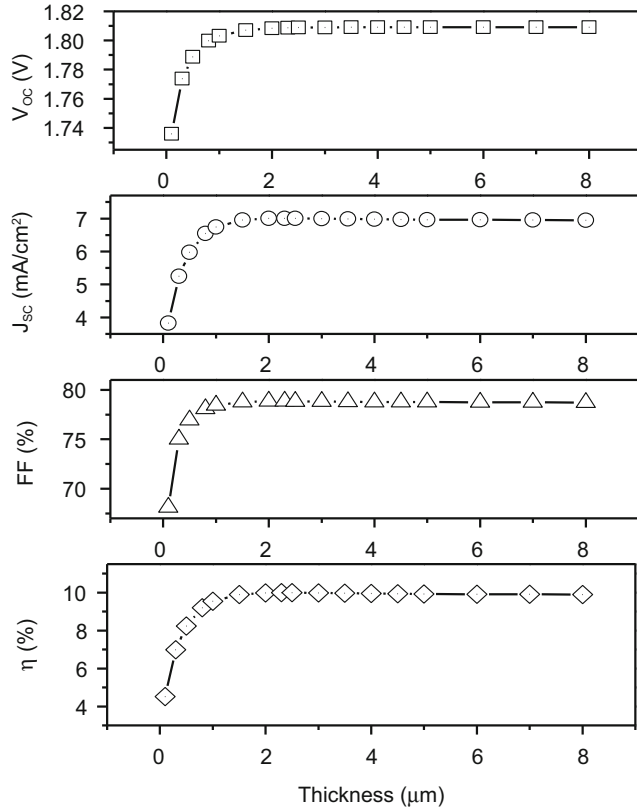


Fig. 5. Photovoltaic characteristics of ZnTe based solar cell as a function of ZnTe layer thickness.

on photovoltaic characteristics was carried out. The ZnTe thickness was varied from 0.1 to 8 μm and the obtained results are shown in Figure 5. One can observe that conversion efficiency η , short-circuit density J_{sc} and fill factor FF increased with increasing the ZnTe thickness up to 2 μm and then it decreased slightly when ZnTe thickness ranged 2 to 8 μm . For the open-circuit voltage V_{oc} , it increased

Table 2. Output parameters of the modelled ZnO/CdS/ZnTe solar cell.

V_{oc} (Volt)	J_{sc} (mA/cm^2)	FF (%)	η (%)
1.81	7.01	78.84	10

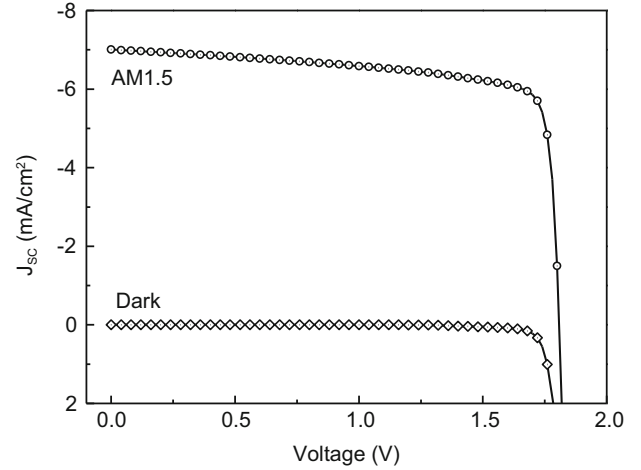


Fig. 6. Dark and illuminated J - V curves of ZnTe based solar cell for ZnTe optimum thickness (2 μm).

continually with ZnTe thickness up to 5 μm and then it has become constant for thickness values above 5 μm . Respect to this behaviour the ZnTe optimum thickness can be considered about 2 μm and the conversion efficiency η , the open circuit voltage V_{oc} , the short circuit current density J_{sc} and the fill factor FF at this optimum thickness are 10%, 1.81 V, 7 mA/cm^2 and 78.84% respectively. Increasing the ZnTe thickness above 2 μm affects slightly the main output parameters of the modelled ZnO/CdS/ZnTe device by a minor decreasing of its values due both to the increasing of the resistance of ZnTe absorber and recombination losses which take place at different layer interfaces and at back contact.

The simulation calculations revealed that the optimal conversion efficiency was about 10% for ZnTe thickness close to 2 μm . Despite the economy of absorber material and the elimination of cadmium element realized in this work the optimal conversion efficiency is lower than that found by Amin et al. [12] relative to the CdTe absorber. They realized a numerical study on the photovoltaic performance of CdS/CdS_{1-x}Te_x/CdTe device and have found the conversion efficiency around 15.5% for CdTe thickness about 2 μm . The difference between the obtained conversion efficiency values is due to various reasons, among others: the gap of CdTe (1.5 eV) is lower than that of ZnTe (2.23–2.28 eV) and recombination losses which take place at different layer interfaces and at back contact. So to improve the conversion efficiency we have to reduce the recombination losses by insertion of a material film to the absorber layer to produce a back surface field and/or doping ZnTe layer by oxygen element to realize ZnTe:O intermediate band semiconductor solar cell (IBSCs).

Doping ZnTe with oxygen element introduces an intermediate band within ZnTe bandgap and enhance the absorption process by exploiting photons of solar spectrum with energy lower than the ZnTe bandgap as shown in the literature [5,7,9].

The photovoltaic parameters of the modelled ZnO/CdS/ZnTe solar cell at the ZnTe optimal thickness ($2\ \mu\text{m}$) are shown in Table 2.

The $J_{\text{sc}}-V$ curves of the ZnTe based solar cell at the dark and under illumination AM1.5 for the ZnTe optimum thickness are plotted in Figure 6. At the dark, the current-voltage curve is typical of Schottky diode. Under illumination the curve shifts toward the higher current values indicating that charge carriers are produced by incident photons. As light density increases the shift is made towards values of current more raised with a steep however more reduced to reach finally saturation.

6 Conclusion

The present work reported on modelling ZnTe based solar cell and a numerical study of the effect of ZnTe absorber thickness on the different output parameters of the proposed ZnO/CdS/ZnTe solar cell device. It was found that the dark $J-V$ characteristic is typical of a Schottky diode. Under illumination the current density increased up to $7\ \text{mA}/\text{cm}^2$ when ZnTe thickness increased up to $2\ \mu\text{m}$ and then it decreased for ZnTe thickness values more than $2\ \mu\text{m}$. Furthermore, as the ZnTe absorber layer decreased the wavelength spectral response decreased also and there is an insufficient absorption for the thinner ZnTe films. It was found that all main characteristics of the modelled solar cell increased with increasing ZnTe thickness up to $2\ \mu\text{m}$ and then decreased for ZnTe thickness ranging $2-8\ \mu\text{m}$ indicating that the ZnTe optimum thickness is about $2\ \mu\text{m}$. At this optimum thickness, conversion efficiency η , open circuit voltage V_{oc} , short circuit current density J_{sc} and fill factor FF are 10%, 1.81 V, $7\ \text{mA}/\text{cm}^2$ and 78.84% respectively. Despite the economy of material shown here the conversion efficiency remains lower. Efforts must be done to enhance this output parameter

by studding factors which allow to reduce recombination losses at layer interfaces and back contact (i.e., reflection, insertion of a material film to the absorber layer for produce a back surface field).

References

1. A. Kaneta, S. Adachi, J. Phys. D: Appl. Phys. **33**, 901 (2000)
2. F. Fang, B.E. Mc Candless, R.L. Opila, I.E.E.E. 001258 (2009)
3. A. Pistone, A.S. Arico, P.L. Antonucci, D. Silvestro, V. Antonucci, Sol. Energy Mater. Sol. Cells **53**, 255 (1998)
4. D.H. Han, J.S. Choi, S.M. Park, J. Electrochem. Soc. **150**, C342 (2003)
5. A. Luque, A. Martí, Phys. Rev. Lett. **78**, 5014 (1997)
6. S. Dhomkar, U. Manna, L. Peng, R. Moug, I.C. Noyan, M.C. Tamargo, I.L. Kuskovsky, Sol. Energy Mater. Sol. Cells **117**, 604 (2013)
7. W. Wang, A.S. Lin, J.D. Phillips, Appl. Phys. Lett. **95**, 011103 (2009)
8. G.L. Araújo, A. Martí, Sol. Energy Mater. Sol. Cells **33**, 213 (1994)
9. A. Luque, A. Martí, Prog. Photovolt. **9**, 173 (2001)
10. A. Luque, A. Martí, Adv. Mater. **22**, 160 (2010)
11. N. Amin, T. Isaka, A. Yamada, M. Konagai, Sol. Energy Mater. Sol. Cells **67**, 195 (2001)
12. N. Amin, K. Sopian, M. Konagai, Sol. Energy Mater. Sol. Cells **91**, 1202 (2007)
13. B.L. Williams, J.D. Major, L. Bowen, L. Philipps, G. Zoppi, I. Forbes, K. Durose, Sol. Energy Mater. Sol. Cells **124**, 31 (2014)
14. M. Burgelman, P. Nollet, S. Degrave, Thin Solid Films **361-362**, 527 (2000)
15. H. Ullah, B. Marí, Superlattices Microstruct. **72**, 148 (2014)
16. O. Skhouni, A. El Manouni, M. Mollar, R. Schrebler, B. Marí, Thin Solid Films **564**, 195 (2014)
17. W. Shockley, W.T. Read, Phys. Rev. **87**, 835 (1952)
18. Z. Fan, J.G. Lu, J. Nanosci. Nanotechnol. **5**, 1561 (2005)
19. D. Verity, F.J. Bryant, C.G. Scott, D. Shaw, Solid State Commun. **46**, 795 (1983)